**ORIGINAL ARTICLE**

# Development of laboratory-cooked, water-resistant, and high-performance Cu-MOF: an economic analysis of Cu-MOF for PFOS pollution management and remediation

Abdelfattah Amari[1] · Ahmad Ismael Saber[2] · Haitham Osman[1] · Velibor Spalevic[3,4] · Branislav Dudic[5,6]

## Abstract

Water pollution is a pressing global concern, with per- and polyfluoroalkyl substances (PFAS) being considered as "forever contaminants." Among them, perfluorooctanesulfonic acid (PFOS) has received significant attention for its adverse effects on human health and aquatic ecosystems. This study aimed to design an innovative adsorbent for effective PFOS removal with exceptional water stability, improving its cost-performance trade-off. The current work simultaneously improved the stability of water of Cu-based metal–organic framework (CMOF) and increased its PFOS removal capacity by modifying it with amine-functionalized $SiO_2$ nanoparticles (AF-CMOF). AF-CMOF presented a lower specific surface area of 999 $m^2\ g^{-1}$ compared to CMOF with a surface area of 1098 $m^2\ g^{-1}$. AF-CMOF showed remarkable PFOS uptake performance of 670 mg/g compared to the performance of the Cu-based MOF which exhibited a PFOS uptake capacity of only 22 mg/g. The most suitable pH for PFOS removal using both adsorbents was determined to be 3. In addition, AF-CMOF demonstrated excellent water stability, retaining its structural integrity even after seven days of water contact, while CMOF structure collapsed rapidly after four days of water exposure. Moreover, the study identified the significant pH influence on the PFOS uptake process, with electrostatic interactions between protonated amine functionalities and PFOS molecules identified as the dominant mechanism. The study's findings present the potential of synthesized adsorbent as a superior candidate for PFOS uptake and contribute to the development of effective water treatment technologies.

**Keywords** Adsorption · PFOS pollution management · Metal–organic framework (MOF) · Water treatment

## Introduction

Over the last few years, concern has grown over time among scientists regarding the issue of environmental pollution (Ly and El-Sayegh 2023, Mousazadeh et al. 2024, Yu et al. 2024a, b). However, the ongoing process of industrialization has continued, resulting in the pollution of the environment, especially water sources (Liu et al. 2023; Xu et al. 2023; Wang et al. 2024a, b). The imperative to control environmental pollution is paramount due to its profound implications for ecological integrity, public health, and sustainable development initiatives (Bozorgnezhad et al. 2015c, a, b;

✉ Branislav Dudic
  branislav.dudic@fm.uniba.sk

  Abdelfattah Amari
  abdelfattah.amari@enig.rnu.tn

  Ahmad Ismael Saber
  ahmad.smael@alnoor.edu.iq

  Haitham Osman
  Haman@kku.edu.sa

[1] Department of Chemical Engineering, College of Engineering, King Khalid University, 61411 Abha, Saudi Arabia

[2] Department of Dentistry, Al-Noor University College, Nineveh, Iraq

[3] Biotechnical Faculty, University of Montenegro, 81000 Podgorica, Montenegro

[4] Faculty of Philosophy, Geography, University of Montenegro, 81400 Niksic, Montenegro

[5] Faculty of Management, Comenius University Bratislava, Bratislava 81499, Slovakia

[6] Faculty of Economics and Engineering Management, University Business Academy, Novi Sad 21000, Serbia

Jiang et al. 2022; Liu et al. 2022; Kong et al. 2023; Xue et al. 2023a, b). Leveraging renewable energy sources holds significant potential for mitigating environmental pollution (Ashrafi et al. 2016; Liu and Yang 2022; Yan et al. 2023). Hence, numerous studies are conducted on renewable energy as a substitute for conventional fuels (Bozorgnezhad et al. 2014; Hussaini and Wang 2022; Kennedy et al. 2023). For renewable energy, various technologies play a pivotal role. Battery storage systems are crucial for storing and managing energy from intermittent sources, ensuring a stable and reliable supply (Bozorgnezhad et al. 2015c, a, b; Bozorgnezhad et al. 2016). Solar energy technologies, including photovoltaic panels and solar thermal systems, harness sunlight to generate electricity and heat (Verma et al. 2024). These advancements in renewable energy not only reduce dependence on fossil fuels but also contribute significantly to sustainable development and the mitigation of climate change (Fatemi et al. 2023; Li et al. 2023a, b).

Furthermore, effective water management practices can yield favorable outcomes for environmental cleanliness (Bozorgnezhad et al. 2015c, a, b). Water resources play diverse roles in various industrial processes, underscoring the critical importance of water management in contemporary times (Hasheminasab et al. 2014; Kanani et al. 2015; Song et al. 2023; Zhao et al. 2024). Water sources encounter a notable obstacle as a result of widespread presence of harmful contaminations particularly per- and polyfluoroalkyl substances (PFAS) (Brusseau et al. 2020; Xu et al. 2023; Xue et al. 2023a, b). Among the various PFAS pollutants, perfluorooctanesulfonic acid (PFOS) has gained great attention because of its utilization in a broad range of industries (Gole et al. 2018). The widespread use of PFOS in industries such as textiles and equipment manufacturing has resulted in its presence in drinking water, municipal sewage, and surface water (Gole et al. 2018). PFOS is highly resistant to natural processes, conventional water treatment techniques, and biodegradation, making it a persistent contaminant in the aquatic system (Erkoç and Erkoç 2001). Moreover, water pollution especially PFOS exposure has been linked to adverse effects on fertility, liver, and the immune system (Espartero et al. 2022; Fatima et al. 2023, Gupta et al. 2023). As such, there is an immediate need to create innovative methodologies for combating PFOS contamination in water sources.

Numerous strategies have been recently looked at ways to lessen the negative impacts of pollutants. Numerous strategies encompass a diverse array of methodologies, including adsorption, electrochemistry, membrane, and sonochemistry (Liu et al. 2008; Lyu et al. 2020; Shen et al. 2023). However, complete eradication of PFAS presents a significant challenge due to its intricate physicochemical properties, which encompass varying chain lengths and substitutions of hydrogen with fluorine atoms (Rayne and Forest 2009).

Owing to the robust carbon–fluorine (C-F) bonds and extensive fluorination, PFAS exhibits remarkable resistance to degradation, along with oleophobic and hydrophobic characteristics, as well as exceptional thermal stability (Gao and Chorover 2012). Biological techniques exhibit the capacity to break carbon–carbon bonds but are limited in their ability to break carbon–fluorine bonds (Zhang et al. 2022). In contrast, oxidation methods like electrochemical oxidation can be employed for PFAS degradation. However, the generation of toxic by-products that are more resistant hinders its widespread application (Ahmed et al. 2020). Hence, the effective elimination of these newly formed smaller PFAS compounds from the water environment poses a new challenge when employing oxidative methods for treating long-chain PFAS compounds (Mirabediny et al. 2023). On the other hand, sorption methods offer the advantage of removing contaminants from water without requiring their degradation (Leung et al. 2022; Yu et al. 2024a, b).

Numerous studies have been carried out on various adsorbents, including activated carbon, clay, and carbon-dot hydrogels, to address the challenge of PFOS removal from water environments (Das et al. 2013; Ross et al. 2018; Wang et al. 2024a, b). However, these adsorbents have inherent limitations in terms of selectivity, efficiency, and kinetics, prompting the need for innovative and sophisticated approaches (Liu et al. 2018; He et al. 2021; Chang et al. 2022). Among the promising alternatives, MOFs have been introduced as a highly encouraging solution for PFOS elimination (Chang et al. 2022). The coordination interactions between organic ligands and metal clusters enable the creation of customizable structures with efficient active sites, superior porosity, and exceptional surface areas (Mohammadi et al. 2021; Li et al. 2023a, 2023b; Li et al. 2024). Consequently, MOFs have gained significant attention for their numerous, exciting uses among a wide range of fields (Han et al. 2022; Hamoule et al. 2023). Despite their exceptional potential, many MOFs have certain drawbacks that limit their practical applications, such as inadequate thermal and water durability (Burtch et al. 2014, Guo et al. 2023). The insufficient water durability of MOFs is a major drawback for their use in actual water refining practices, since extended exposure to water can cause structural deterioration (Ding et al. 2019; Yu et al. 2024a, b). The primary influences on MOFs' water resistance are steric and electrical hindrance effects on the metal cluster, which can weaken the metal–ligand coordination (Ding et al. 2019). In order to make MOFs water tolerant, the metal cluster's inertness is an essential structural feature that inhibits the deterioration process (Wang et al. 2016). To address the issue of weak water stability, one promising approach is to propose modification methods that can enhance the water tolerance of MOFs (Yang et al. 2019). Furthermore, enhancing the structural stability of MOFs has cost efficiency implications.

A techno-economic analysis of MOFs demonstrated that the production cost at an industrial scale ranges from 35 to 71 dollars (DeSantis et al. 2017). This high cost currently limits the widespread application of MOFs in real-world scenarios. However, if MOFs can exhibit prolonged stability in water for water treatment applications, it can significantly improve their cost-performance trade-off efficacy.

In recent years, surface modification techniques have gained attention as a viable approach for enhancing the water stability of MOFs (Weiss et al. 2015). This method involves modifying the MOF's surface by introducing steric hindrance on metal centers, which obstructs water molecules from accessing the metal centers and ultimately leading to their degradation (Liu et al. 2014). By applying a PDMS layer by vapor deposition, researchers have successfully enhanced the water stability of MOFs such as HKUST-1, MOF-5, and ZnBT. This has led to noticeably enhanced resilience for a maximum of one day of water exposure (Zhang et al. 2014). Additionally, studies by Lin et al. have showed that modifying the metal nodes of acetonitrile functionalization Cu-BTC can significantly enhance water resistance, extending its performance for as long as 20 days (Lin et al. 2018). These findings have opened up new avenues for further research into surface modification techniques in order to improve MOF's water stability. Moreover, surface modification is a critical aspect of improving the performance of MOFs for various uses, including pollutant removal (Lv et al. 2019). Through surface modification, MOFs can be tailored to have enhanced surface functionalities, leading to higher adsorption capacity (Pauletto et al. 2023). The electrostatic driving force among the electrophobic head of PFOS and cationic functional groups of the sorbent has been found as a promising mechanism for PFOS removal. Studies have revealed that aminated polyacrylonitrile fibers with protonated amine functionalities at pH 3 for PFOS exhibit remarkable adsorption capacities of up to 15.0 mmol/g owing to the strong electrostatic forces among the positively charged amine groups and the anionic PFOS headgroup (Meng et al. 2017). Similarly, triazine- and heptazine-based porous organic polymer networks have shown excellent adsorption of PFOA by utilizing the electrostatic interactions among nitrogen groups within the polymer framework and PFOA particles (Abdullatif et al. 2022).

As the Cu-based MOF has become commercially available, a method is sought to enhance its stability in water and make it appropriate for practical uses in water treatment. Cu-based MOF, unlike certain other MOFs, has metal nodes facing the inner pore space, which render them susceptible to water attacks. To overcome this challenge, this study aims to immobilize $NH_2$-$SiO_2$ nanoparticles onto CMOF, which serves a dual purpose of increasing steric hindrance on the metal sites and introducing $NH_2$ functionalization onto the adsorbent to improve PFOS adsorption capacity.

By doing so, the accessibility of water to the metal centers within CMOF is notably impeded, making it more stable in aqueous environments and more effective at removing PFOS. The morphological attributes and water resistance of the synthesized adsorbent were examined using nitrogen adsorption–desorption pattern, Fourier transform infrared (FTIR) spectroscopy, X-ray diffraction (XRD) analysis, and scanning electron microscopy (SEM) methods. The experimental conditions, which play a crucial role in PFOS adsorption, were evaluated such as pH level of the water, PFOS content, process time, and reusability of the adsorbent, as well as isothermal and kinetic studies.

# Experiments and methodology

## Chemicals

The reagents used in this research were obtained from sources such as Sigma-Aldrich and Merck companies, and were used without any additional purification. The chemical substances included 3-aminopropyl triethoxysilane (APTS), silicon dioxide nanopowder, benzene-1,3,5-tricarboxylic acid, hydrochloric acid, cupric nitrate trihydrate, sodium hydroxide, and ammonia aqueous solution.

## Synthesis of adsorbents

To synthesize CMOF, two distinct solutions denoted as (A) and (B) were prepared. Solution (A) was composed of 3.15 g of trimesic acid ($H_3BTC$) dissolved in 90 mL of ethanol, while solution (B) comprised 6.522 g of copper nitrate trihydrate ($Cu(NO_3)_2 \cdot 3H_2O$) dissolved in 90 mL of distilled water. These solutions were subsequently combined under continuous agitation for a duration of 45 min. The resulting mixture was transferred into a stainless-steel autoclave, securely sealed, and subjected to a heating process lasting 12 h at 120 °C. Following the completion of the reaction, the resulting product underwent a washing procedure utilizing distilled ethanol and water, followed by dehumidification at 150 °C for a period of one day. The synthesized material was designated as CMOF. For the synthesis of $NH_2$-$SiO_2$ nanoparticles, a solution comprising 280 mL ethanol and distilled water was prepared, and 2.2 mL of concentrated ammonia solution and 1 g of $SiO_2$ NPs were added. Simultaneously, 2.25 g of APTS was introduced gradually into the stirring mixture over a 6-h period. Following centrifugation, the resulting mixture underwent purification through successive washes with deionized water and ethanol, followed by dehydration at 60 °C for 10 h. To synthesize the modified CMOF, a blend of 45 mL of DMF and ethanol (1:1 by volume) with 1.575 g of trimesic acid ($H_3BTC$) was prepared. Following this, 0.11 g of amine-functionalized silica

nanoparticles (NH2-SiO2 NPs) and 10 mL of ethanol were added to the mixture, which was then heated to 70 °C. Subsequently, 45 mL of deionized water containing 3.261 g of copper nitrate trihydrate (Cu (NO₃)₂·3H₂O) was introduced, and the entire solution was agitated for a duration of four hours. The resulting mixture was transferred to a stainless-steel autoclave and subjected to 12 h of heating at 120 °C in an oven. Following centrifugation and subsequent ethanol washing, a white powder termed AF-CMOF was obtained. This powder was then preserved for future applications.

## PFOS adsorption test

In the current work, batch-scale experiments were carried out to examine the ability of CMOF and AF-CMOF to adsorb PFOS from aqueous solutions. Specifically, 140 mg/L dosage of the synthesized adsorbents was introduced into 50 mL of PFOS solution, with concentrations varying from 10 to 100 mg/L. Subsequently, the blend was agitated for a duration of three hours, and then, the adsorbent particles were removed through centrifugation. The remaining PFOS content was measured using LS-MS analysis. The capacity of CMOF and AF-CMOF for PFOS removal was evaluated using the following equations:

$$\text{PFOS adsorption capacity} = q_e = (C_i - C_e) \times \frac{V}{m}$$

$$\text{PFOS adsorption percentage} = (C_i - C_f) \times \frac{100}{C_i}$$

Here, the initial PFOS content in the aqueous solution was represented by $C_i$ (mg/L), while the concentration after the adsorption process was designated as $C_f$ (mg/L). The total volume of the samples was denoted as $V$ (in L), and the amount of adsorbent used for treatment was represented by $m$ (in g).

## Water stability analysis

To determine the water resistance of CMOF and AF-CMOF, samples with a volume of 50 mL containing 100 mg of each adsorbent were prepared. The pH of the samples was fixed to 7, and they were maintained in water for four and seven days, respectively. After each time interval, the samples were characterized to evaluate any changes in their structure. Additionally, the PFOS adsorption capacity of the samples was assessed both before and after a seven-day exposure to water.

# Results and discussion

## Characterization

XRD spectra were obtained for both AF-CMOF and CMOF, and the findings are presented in Fig. 1. The XRD results of CMOF showed distinctive peaks at $2\theta$ angles of 4.6°, 6.4°, 9.8°, 10.5°, 12.6°, 14.1°, 16.2°, 17.9°, 18.6°, 19.5°, 21.8°, 24.5°, and 25.9°, suggesting that the crystalline structure of the MOF was successfully formed. The alteration had no impact on the crystalline structure of CMOF, as substantiated by the reduction in intensity of certain peaks and the observation of minor shifts (Ke et al. 2011). Specifically, the peak at $2\theta = 9.8°$ shifted to 9.9°, and the peak at $2\theta = 10.5°$ shifted to 10.4°. Following immersion in water for four and seven days, the intensity of the characteristic peaks for CMOF notably diminished, while new peaks emerged at approximately 10°, signifying the degradation of the crystalline structure upon water contact. The intensity of peaks was only slightly reduced for AF-CMOF, and the peak positions were mostly preserved, suggesting that the sample's
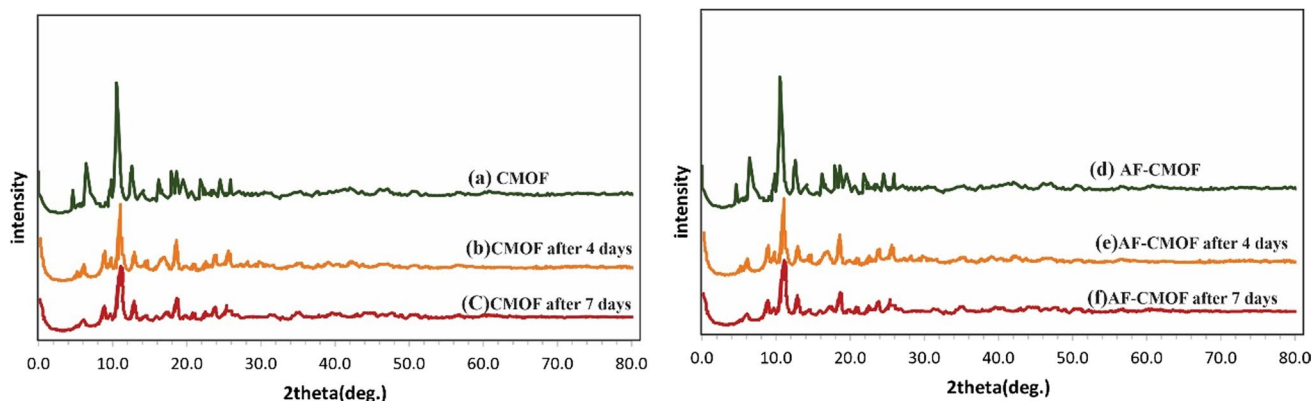


**Fig. 1** XRD pattern of **a** CMOF, **b** CMOF following four days of water exposure, **c** CMOF following seven days of water exposure, **d** AF-CMOF, **e** AF-CMOF following four days of water exposure, **f** AF-CMOF following seven days of water exposure

crystallinity remained intact even after being in contact with water molecules for seven days.

The morphological characteristics of both CMOF and AF-CMOF were examined using the FE-SEM technique. As conveyed in Fig. 2, the CMOF showcases an octahedral configuration, featuring the typical particle size of 13.90 µm. After modification with $NH_2$-$SiO_2$ nanoparticles, the MOF morphology shifted from a regular octahedral framework to an irregular one. It also presents a comparison of SEM images of both samples prior and post water contact (Fig. 2). It was evident that prolonged contact with the aqueous environment led to the loss of CMOF's crystalline structure. In contrast, AF-CMOF exhibited only a minor reduction in crystallinity following exposure to water. These SEM images align with the observations made from the XRD patterns. In Fig. 2, an EDS map of AF-CMOF reveals the presence of
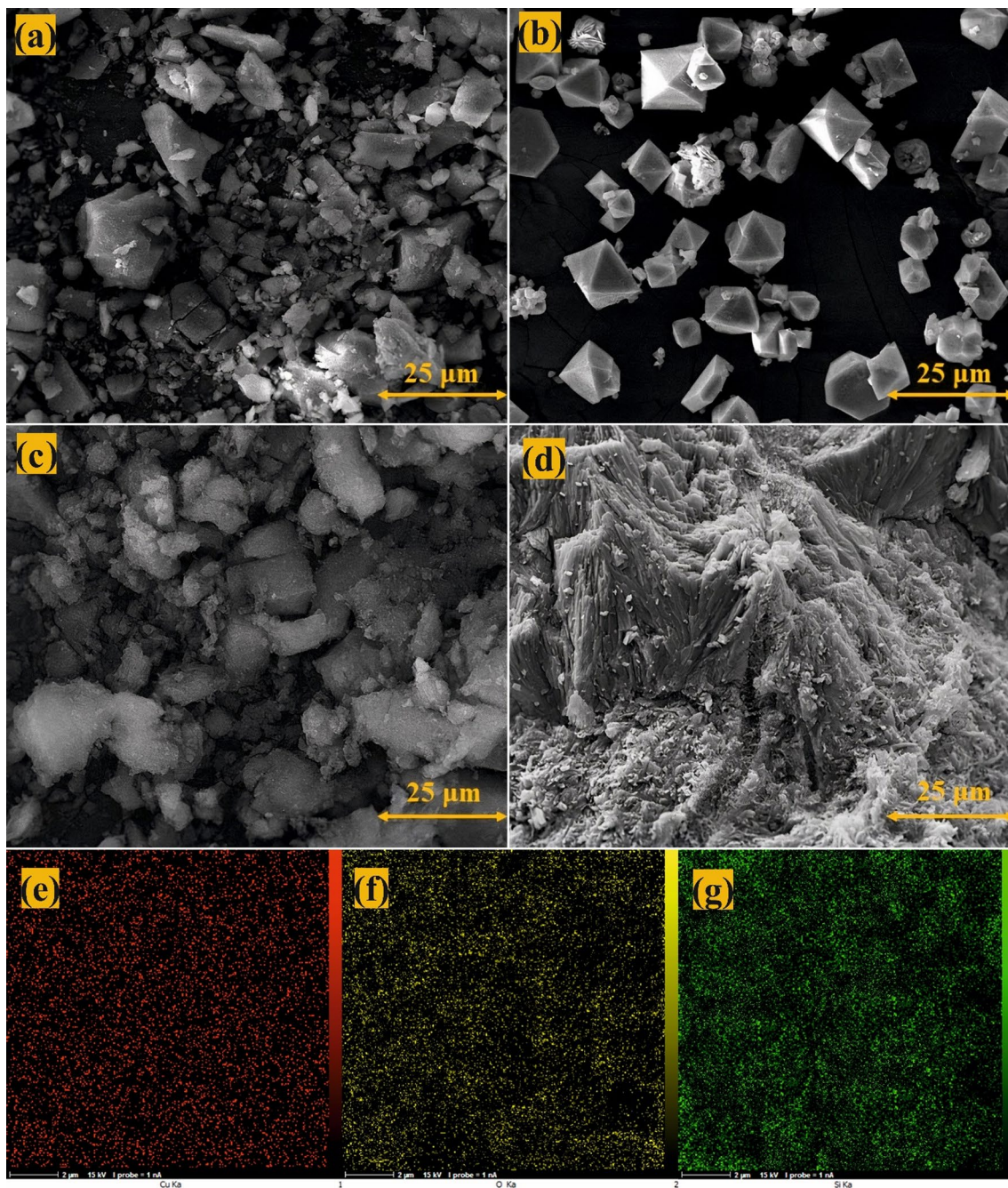


**Fig. 2** **A** SEM image of CMOF (10 µm), **B** SEM image of CMOF (200 nm), **C** SEM image of AF-CMOF (10 µm), **D** SEM image of AF-CMOF(200 nm)

**Table 1** Textural features of AF-CMOF and CMOF

| Adsorbent | $S_{BET}$ (m$^2$/g) | Total pore volume (cm$^3$/g) |
|---|---|---|
| CMOF | 1098 | 0.67 |
| AF-CMOF | 999 | 0.52 |

Si, Cu, and O atoms. The uniform distribution of N and Si atoms within the AF-CMOF structure, positioned near the Cu atoms, underscores the role of $NH_2$-$SiO_2$ nanoparticles in creating a barrier against water penetration.

Table 1 displays the structural features of both AF-CMOF and CMOF. Nitrogen adsorption isotherms were employed to evaluate the pore size distribution and surface area. All samples showcased a Type I isotherm, indicating the existence of micropores and mesopores. Both materials had a high surface area, with the CMOF having a surface area of 1098 m$^2$/g according to Fig. 3. However, after the modification of the CMOF with $NH_2$-$SiO_2$, the surface area of AF-CMOF was slightly decreased to 999 m$^2$/g according to Fig. 3. Based on Fig. 4, the pore volume of AF-CMOF was also found to be lower than that of CMOF, indicating that the surface coverage using $NH_2$-$SiO_2$ particles has occurred.

Figure 5 presents a comparison of the FTIR results of AF-CMOF and CMOF. Both samples showed similar profiles, indicating that the modification with $NH_2$-$SiO_2$ nanoparticles did not alter the structure of the CMOF. This observation aligns with the outcome derived from the XRD results. The identification of C=O and C–H was observed at 1645 cm$^{-1}$ and 2936 cm$^{-1}$, respectively; also, O–H, C–O–, and –O– groups were identified at peaks around 3500, 1431, and 1583 cm$^{-1}$, respectively



**Fig. 3** Nitrogen sorption–desorption isotherms for both AF-CMOF and CMOF
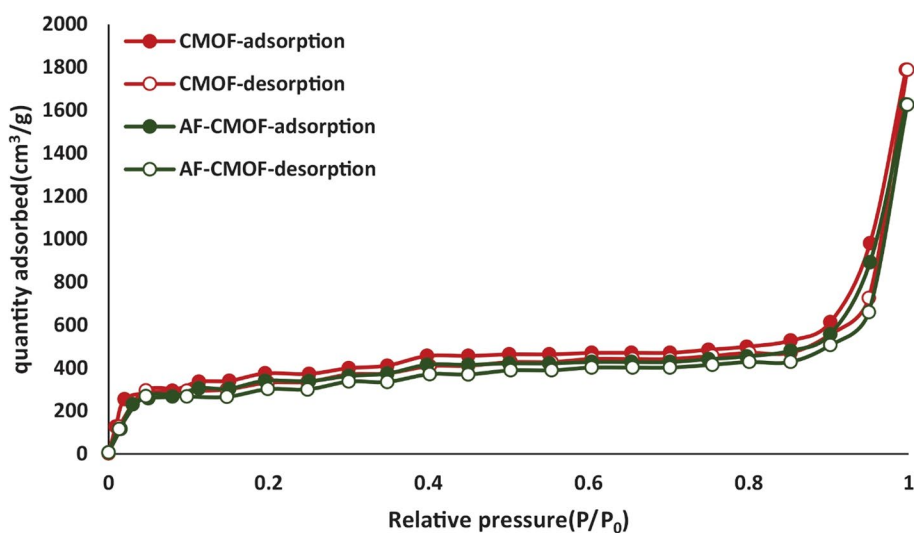


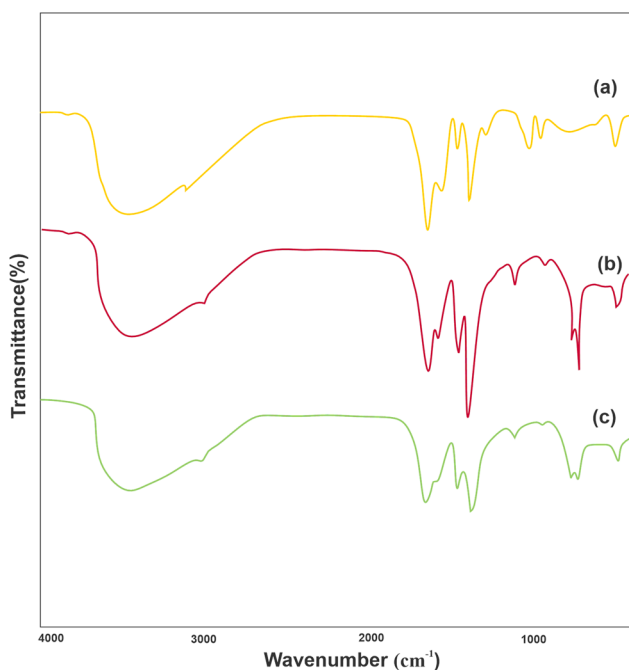**Fig. 4** Pore size distribution of AF-CMOF and CMOF
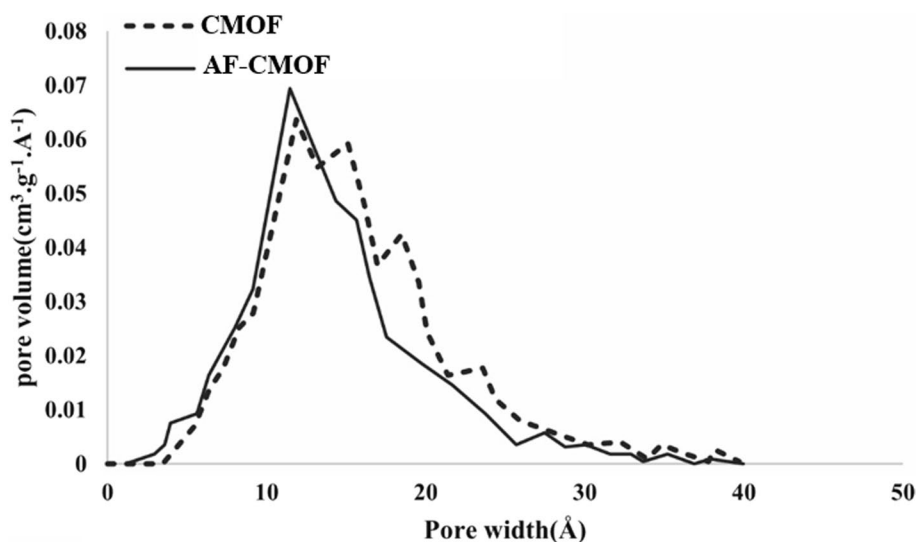
**Fig. 5** FTIR results of **a** CMOF, **b** AF-CMOF, and **c** AF-CMOF after adsorption

(Madden et al. 2022). Additionally, the FTIR spectrum of AF-CMOF demonstrated some characteristic peaks of $NH_2$-$SiO_2$, including Si–O-Si at approximately 1036 cm$^{-1}$ and Si–O at around 808 cm$^{-1}$. Also, C–N stretches were observed at 1257 and 1340 cm$^{-1}$ and N–H bending was identified at 764 cm$^{-1}$ (Bhoria et al. 2020).

## Assessment of PFOS adsorption onto CMOF and AF-CMOF

The effectiveness of CMOF and AF-CMOF in PFOS removal after exposure to water for four and seven days was examined in this study. As mentioned in Fig. 6, CMOF showed a significant reduction in its PFOS adsorption performance after only four days of contact with water, with the adsorption capacity dropping to a mere 2 mg/g. After seven days, CMOF exhibited almost no adsorption capacity. In contrast, AF-CMOF demonstrated remarkable water stability, retaining 89% of its initial PFOS adsorption capacity even after seven days of water exposure. These results indicate that AF-CMOF has exceptional water resistance compared to CMOF. Moreover, the aim of this section was to evaluate the PFOS elimination using CMOF and AF-CMOF via analyzing Freundlich and Langmuir isotherm equations in addition to pseudo-first- and second-order models to investigate the kinetic data. The corresponding equations are given below:
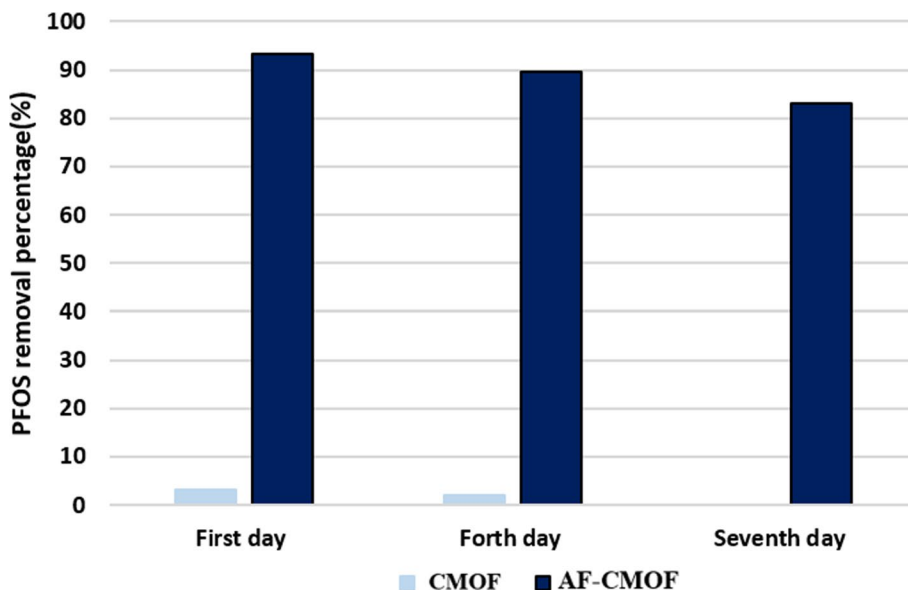
$$1/q_e = 1/(C_e \times q_m \times K_l) + 1/q_m \quad \text{(Langmuir isotherm equation)}$$

$$\text{Log } q_e = \text{Log } K_f + 1/n \times \text{Log } C_e \quad \text{(Freundlich isotherm equation)}$$

$$\text{Ln}(q_m - q_t) = \text{Ln } q_m - K_1 \times t \quad \text{(pseudo} - \text{first order kinetic equation)}$$

$$t/q_t = 1/K_2 \times q_m^2 + t/q_m \quad \text{(pseudo} - \text{second order kinetic equation)}$$

**Fig. 6** PFOS removal by CMOF and AF-CMOF after four- and seven-day exposure to water

The Langmuir model showed the highest theoretical PFOS uptake performance for CMOF ($R^2 = 0.9975$) and AF-CMOF ($R^2 = 0.999$) according to Fig. 7 and Table 2 to be 24 and 689 mg/g, respectively. Though, the actual highest PFOS adsorption was recorded as 23 mg/g for CMOF and 650 mg/g for AF-CMOF, signifying a lower real PFOS sorption performance for both materials than the theoretical capacity. The PFOS uptake onto adsorbents rapidly achieved the maximum capacity within a time of 25 and 20 min according to Fig. 8 and Table 3 for AF-CMOF and CMOF, respectively. The slight time difference in the equilibrium time might be due to the existence of $NH_2$-$SiO_2$ nanoparticles that confined the pore network of the MOF. PFOS adsorption adhered to the pseudo-second-order model, indicating that the sorption rate is dictated by the chemisorption phase. The Langmuir model demonstrated good agreement with the adsorption isotherms on both CMOF and AF-CMOF, suggesting that the PFOS adsorption took place on a uniform surface with a limited number of equivalent sorption sites. The results highlighted the potential of these MOFs as effective adsorbents for removing PFOS from water environments. It should be mentioned that the AF-CMOF showed a better performance in PFOS removal than most of the similar adsorbents, including magnetic carbon nitride and porous silica adsorbents. For instance, magnetic carbon nitride adsorbent exhibited a PFOS uptake performance of 454.55 mg/g, while porous silica adsorbents exhibited PFOS elimination performance in the range of 70–490 mg/g (Punyapalakul et al. 2013; Yan et al. 2014).

## Assessment of the PFOS removal mechanism and the effect of pH value

The present study extensively examined the pH influence on the PFOS adsorption onto AF-CMOF. The findings proposed that the most effective adsorption of AF-CMOF was
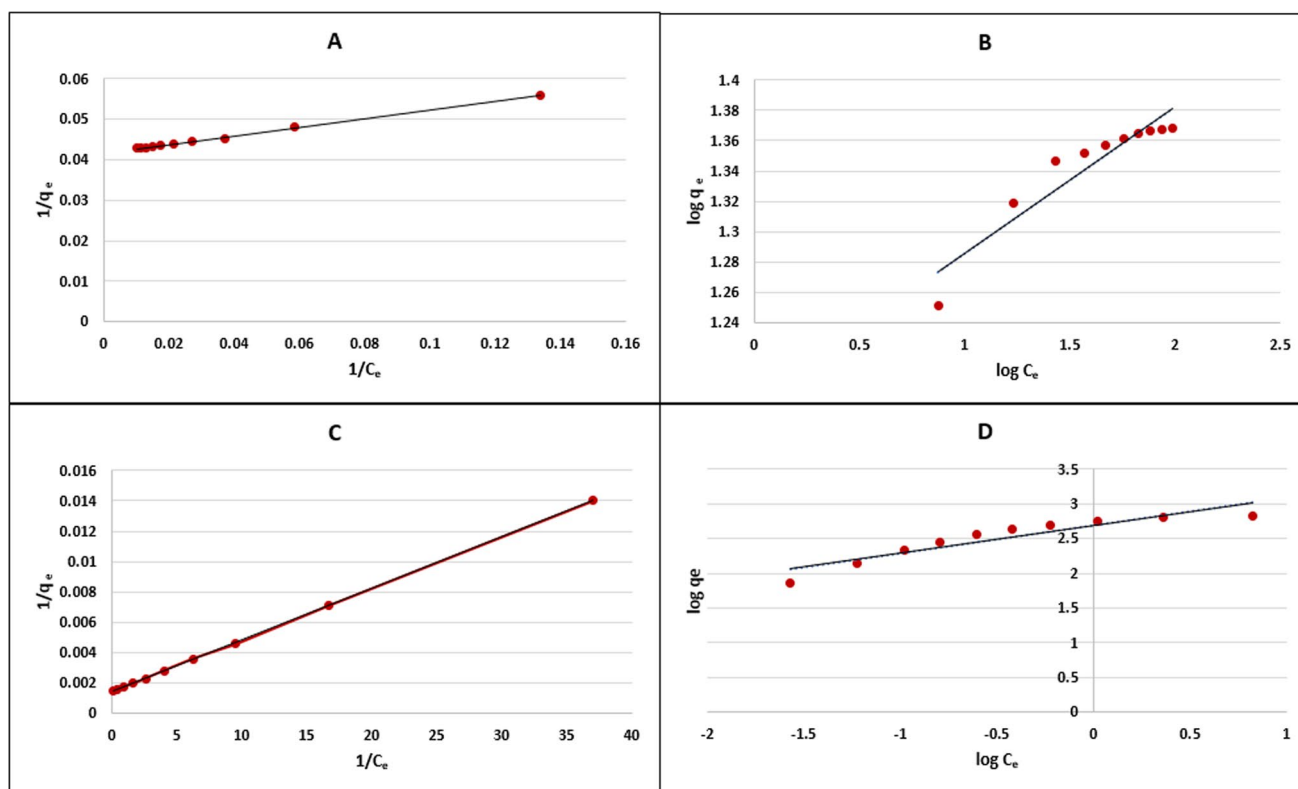


**Fig. 7** **A** Langmuir isotherm of CMOF, **B** Freundlich isotherm of CMOF, **C** Langmuir isotherm of AF-CMOF, **D** Freundlich isotherm of AF-CMOF

**Table 2** Fitting parameters for Langmuir and Freundlich isotherms

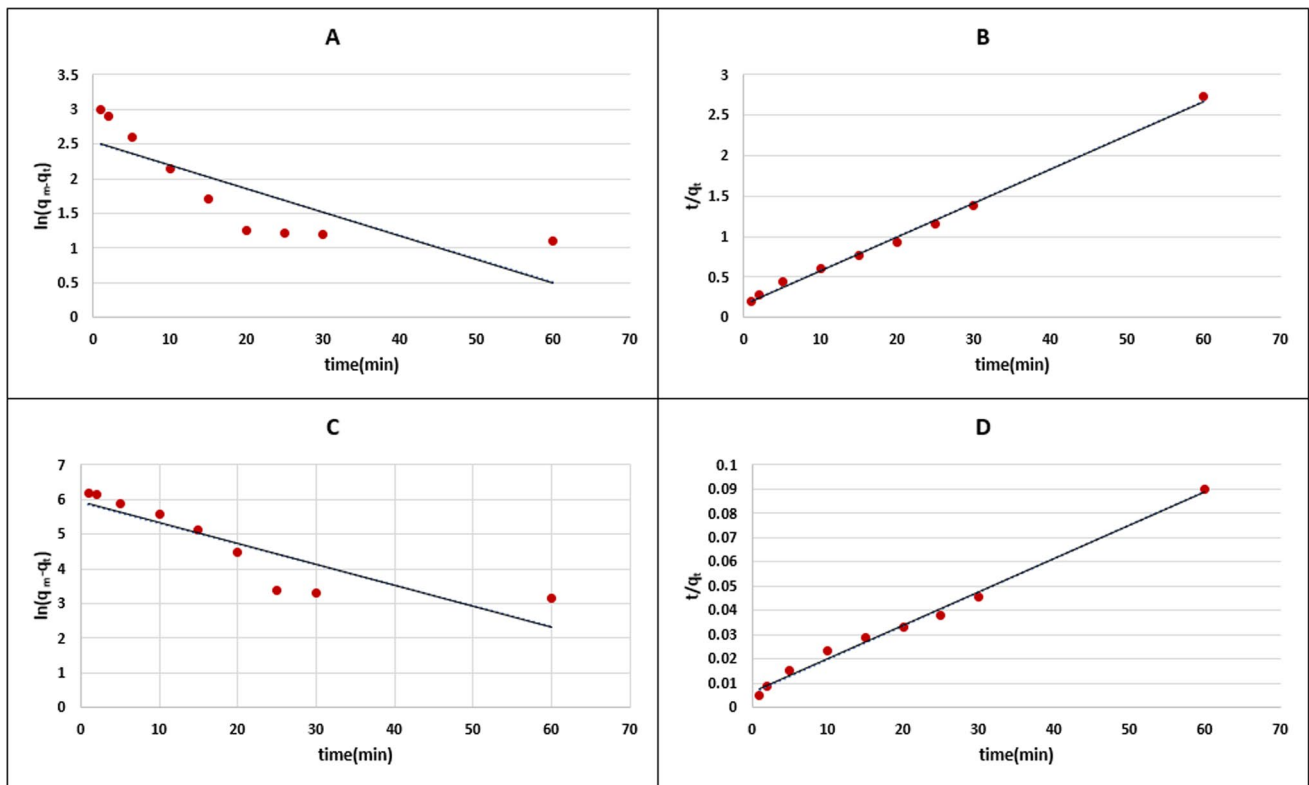|  | Langmuir | | | Freundlich | | |
|---|---|---|---|---|---|---|
|  | $q_m$(mg/g) | $K_l$(L/mg) | $R^2$ | $n$ | $K_f$(mg/g) | $R^2$ |
| CMOF | 24 | 0.4 | 0.9975 | 10.37 | 15.47 | 0.8816 |
| AF-CMOF | 689 | 4.24 | 0.999 | 2.52 | 485.96 | 0.8538 |

**Fig. 8 A** Pseudo-first-order model of CMOF, **B** Pseudo-second-order model of CMOF, **C** Pseudo-first-order model of AF-CMOF, **D** Pseudo-second-order model of AF-CMOF

**Table 3** Calculated parameters from pseudo-first and second-order kinetic equations

| Materials | Pseudo-first-order | | | Pseudo-second-order | | |
|---|---|---|---|---|---|---|
| | $q_m$ (mg/g) | $K_1$ (1/min) | $R^2$ | $q_m$ (mg/g) | $K_2$ (g/mg.min) | $R^2$ |
| CMOF | 12.6 | 0.0339 | 0.6598 | 23.92 | 0.0107 | 0.9962 |
| AF-CMOF | 371.59 | 0.06 | 0.7754 | 714.29 | 0.0003 | 0.9919 |

attained at a pH level of 3, as illustrated in Fig. 9. It could be attributed to the protonation of amine functionalities at acidic pH levels. As a result, the positively charged amine groups create active sites for the sulfonate headgroup of PFOS molecules, facilitating the adsorption process. However, at pH levels exceeding 7, the presence of $OH^-$ ions compete with PFOS during the adsorption process, consequently exerting a detrimental influence on the conditions for PFOS removal. These findings align with previous studies investigating PFOS adsorption through aminated adsorbents, which emphasized the importance of the initial pH value in determining the adsorption efficiency (Zhang et al. 2011a, b; Aly et al. 2019).

To conduct additional research the adsorption mechanism of PFOS onto the AF-CMOF and to determine the specific functionalities participated in the process, an analysis of the FTIR result of the adsorbent sample was conducted

following the adsorption. The intensity of the peaks related to $NH_2$ functionalities, including the C–N stretches at 1257 and 1340 cm$^{-1}$ and the N–H bending band at 764 cm$^{-1}$, reduced after the adsorption of PFOS. This observation demonstrates that the amine functionalities act as a significant role in the PFOS uptake process. The amine functionalities become protonated and obtain a positive charge at low pH values, which allows them to provide electrostatic interactions to capture PFOS. The obtained results are consistent with published literature that have shown the involvement of amine groups in the sorption of anionic PFAS. An instance of this phenomena is the FTIR analysis of cross-linked chitosan adsorbent after PFOS adsorption, which revealed a slight decrease and a shift in the characteristic peaks of N–H groups from 3429 to 3470 cm$^{-1}$ and from 1649 to 1635 cm$^{-1}$, attributed to the N–H stretches and bending, respectively (Zhang et al. 2011a, b; Ateia et al.

**Fig. 9** pH effect on the PFOS adsorption performance at C = 100mg/L
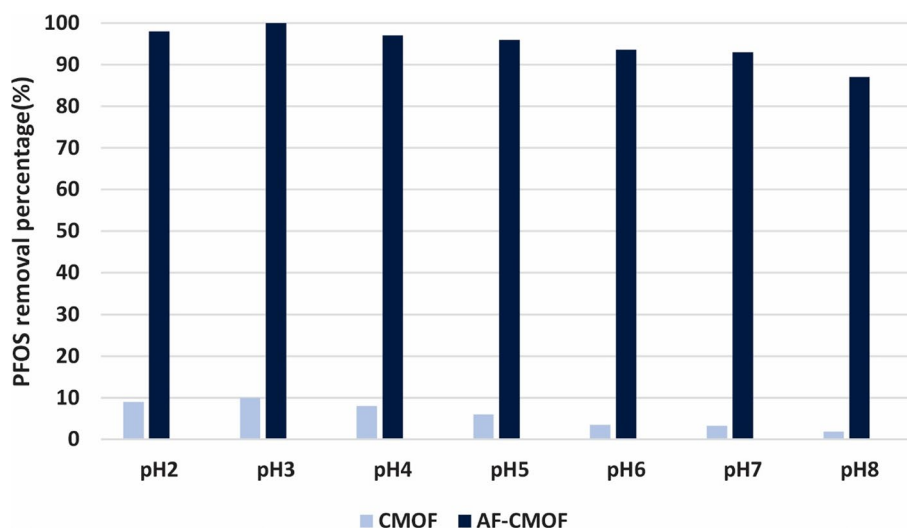


2019). These results suggest that the amine moieties that exist in the adsorbent were in direct interaction with the adsorbed PFOS. In addition, the point of zero charge (PZC) for an adsorbent is the pH at which the solution exhibits constancy despite the introduction of additional acid or base. At this point, the adsorbent carries a neutral charge, and subsequent additions of acid or base have no impact on pH. Accurately determining the PZC is essential for comprehending the adsorbent's behavior and refining its application across diverse scenarios. In the specific instance of AF-CMOF, the point of zero charge was ascertained to be 5.6.

## Assessment of adsorbent reusability

Recovery and reuse of the adsorbent is a critical factor in industrial applications. The potential for reuse of the synthesized MOF was evaluated by performing adsorption/desorption cycles. The obtained results demonstrated that there was a slight decline in the PFOS removal performance after the recovery of adsorbent, which may be related to either the saturation of active sites or the chemical behavior of the adsorption process. Nevertheless, as depicted in Fig. 10, AF-CMOF demonstrated an acceptable capacity for reuse, maintaining 93% of its initial PFOS removal capacity for up to eight cycles. This suggests that AF-CMOF could be a potential candidate for real-life water treatment situations, especially where repeated use is required.

## Conclusion

In conclusion, this study introduces an innovative approach to designing an adsorbent for efficient PFOS removal from water media. Through the modification of a coordination

**Fig. 10** Recovery study of CMOF and AF-CMOF for lead ions adsorption process at pH = 7 and C = 100 mg/L
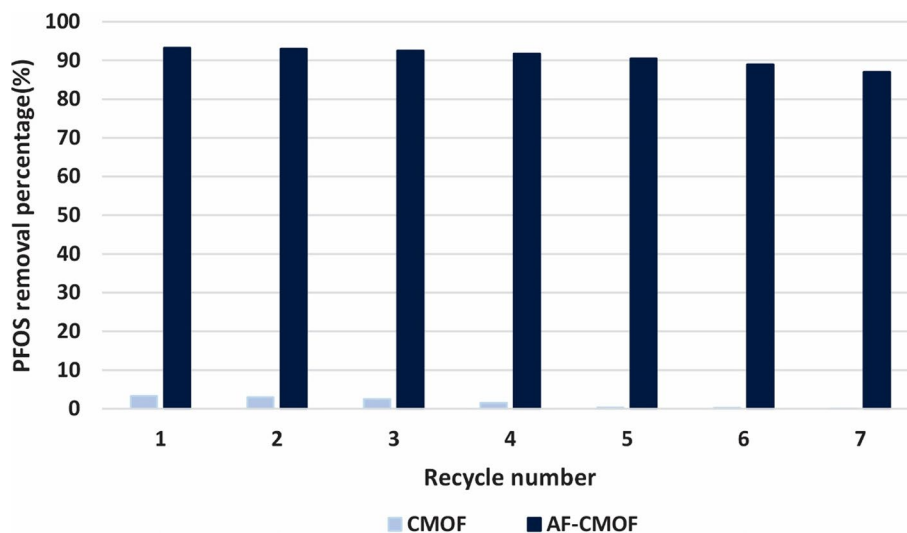
microporous organic framework (CMOF) with amine-functionalized $SiO_2$ nanoparticles, the synthesized product demonstrated an outstanding PFOS uptake capacity of 670 mg/g, surpassing the capacity of the unmodified CMOF by over 30 times. AF-CMOF, despite having a reduced specific surface area of 999 $m^2$ $g^{-1}$ compared to CMOF's surface area of 1098 $m^2$ $g^{-1}$, displayed superior PFOS adsorption characteristics. The PFOS uptake process adhered to a monolayer chemisorption, as indicated by the pseudo-second-order kinetic model and Langmuir isotherm. Additionally, the modified adsorbent exhibited remarkable water stability, maintaining its structural integrity even after seven days of water exposure, unlike CMOF, which experienced rapid collapse after four days of water exposure. The study highlighted the significant impact of solution pH on the PFOS uptake process, emphasizing the dominance of electrostatic interactions between protonated amine functionalities and PFOS molecules. In summary, the findings of this research hold significant implications for the development of highly effective and durable adsorbents for PFOS removal from contaminated water sources.

## Declarations

**Conflict of interest** All authors declare no conflict of interest.

**Ethical approval** The authors did this research in compliance with ethical standards.

## References

Abdullatif D, Khosropour A, Khojastegi A, Mosleh I, Khazdooz L, Zarei A, Abbaspourrad A (2022) Triazine-and Heptazine-based porous organic polymer networks for the efficient removal of perfluorooctanoic acid. ACS Appl Polymer Mater 5(1):412–419

Ahmed MB, Alam MM, Zhou JL, Xu B, Johir MAH, Karmakar AK, Rahman MS, Hossen J, Hasan AK, Moni MA (2020) Advanced treatment technologies efficacies and mechanism of per-and poly-fluoroalkyl substances removal from water. Process Saf Environ Prot 136:1–14

Aly YH, McInnis DP, Lombardo SM, Arnold WA, Pennell KD, Hatton J, Simcik MF (2019) Enhanced adsorption of perfluoro alkyl substances for in situ remediation. Environ Sci: Water Res Technol 5(11):1867–1875

Ashrafi M, Shams M, Bozorgnezhad A, Ahmadi G (2016) Simulation and experimental validation of droplet dynamics in microchannels of PEM fuel cells. Heat Mass Transf 52:2671–2686

Ateia M, Alsbaiee A, Karanfil T, Dichtel W (2019) Efficient PFAS removal by amine-functionalized sorbents: critical review of the current literature. Environ Sci Technol Lett 6(12):688–695

Bhoria N, Basina G, Pokhrel J, Reddy KSK, Anastasiou S, Balasubramanian VV, AlWahedi YF, Karanikolos GN (2020) Functionalization effects on HKUST-1 and HKUST-1/graphene oxide hybrid adsorbents for hydrogen sulfide removal. J Hazard Mater 394:122565

Bozorgnezhad A, Shams M, Kanani H, Hashemi Nasab MR (2014) Experimental study of the effect of inlet flow parameters on the operation of PEMFC. Modares Mech Eng 14(5):33–43

Bozorgnezhad A, Shams M, Kanani H, Hasheminasab M (2015b) Experimental investigation on dispersion of water droplets in the single-serpentine channel of a PEM fuel cell. J Dispersion Sci Technol 36(8):1190–1197

Bozorgnezhad A, Shams M, Kanani H, Hasheminasab M, Ahmadi G (2015c) The experimental study of water management in the cathode channel of single-serpentine transparent proton exchange membrane fuel cell by direct visualization. Int J Hydrogen Energy 40(6):2808–2832

Bozorgnezhad A, Shams M, Kanani H, Hasheminasab M, Ahmadi G (2016) Two-phase flow and droplet behavior in microchannels of PEM fuel cell. Int J Hydrogen Energy 41(42):19164–19181

Bozorgnezhad, A., M. Shams, G. Ahmadi, H. Kanani and M. Hasheminasab (2015). The experimental study of water accumulation in PEMFC cathode channel. Fluids engineering division summer meeting, American Society of Mechanical Engineers.

Brusseau ML, Anderson RH, Guo B (2020) PFAS concentrations in soils: background levels versus contaminated sites. Sci Total Environ 740:140017

Burtch NC, Jasuja H, Walton KS (2014) Water stability and adsorption in metal–organic frameworks. Chem Rev 114(20):10575–10612

Chang P-H, Chen C-Y, Mukhopadhyay R, Chen W, Tzou Y-M, Sarkar B (2022) Novel MOF-808 metal–organic framework as highly efficient adsorbent of perfluorooctane sulfonate in water. J Colloid Interface Sci 623:627–636

Das P, Arias EVA, Kambala V, Mallavarapu M, Naidu R (2013) Remediation of perfluorooctane sulfonate in contaminated soils by modified clay adsorbent—a risk-based approach. Water, Air, & Soil Pollut 224:1–14

DeSantis D, Mason JA, James BD, Houchins C, Long JR, Veenstra M (2017) Techno-economic analysis of metal–organic frameworks for hydrogen and natural gas storage. Energy Fuels 31(2):2024–2032

Ding M, Cai X, Jiang H-L (2019) Improving MOF stability: approaches and applications. Chem Sci 10(44):10209–10230

Erkoç Ş, Erkoç F (2001) Structural and electronic properties of PFOS and LiPFOS. J Mol Struct (thoechem) 549(3):289–293

Espartero LJL, Yamada M, Ford J, Owens G, Prow T, Juhasz A (2022) Health-related toxicity of emerging per-and polyfluoroalkyl

substances: comparison to legacy PFOS and PFOA. Environ Res 212:113431

Fatemi SAZ, Zgham W, Shirzad S, Serat Z (2023). Feasibility study of theoretical efficiency calculation for flat plate collectors in solar water heating systems. Arch Advan Eng Sci, 1–12

Fatima M, Khan MA, Shaheen S, Almujally NA, Wang SH (2023) B2C3NetF2: Breast cancer classification using an end-to-end deep learning feature fusion and satin bowerbird optimization controlled Newton Raphson feature selection. CAAI Trans Intell Technol 8(4):1374–1390

Gao X, Chorover J (2012) Adsorption of perfluorooctanoic acid and perfluorooctanesulfonic acid to iron oxide surfaces as studied by flow-through ATR-FTIR spectroscopy. Environ Chem 9(2):148–157

Gole VL, Fishgold A, Sierra-Alvarez R, Deymier P, Keswani M (2018) Treatment of perfluorooctane sulfonic acid (PFOS) using a large-scale sonochemical reactor. Sep Purif Technol 194:104–110

Guo D, Li H, Xu Z, Nie Y (2023) Development of pyrene-based MOFs probe for water content and investigations on their mechanochromism and acidochromism. J Alloy Compd 968:172004

Gupta S, Shabaz M, Gupta A, Alqahtani A, Alsubai S, Ofori I (2023). Personal healthcare of things: a novel paradigm and futuristic approach. CAAI Trans Intell Technol

Hamoule T, Mohammadi N, Mousazadeh B, Fakhari H (2023) Simultaneous improvement of water stability and performance of HKUST-1 for fast cadmium removal from the water environment: synthesis, characterization, RSM optimization, thermodynamics and kinetics. Int J Environ Sci Technol 20(11):11913–11930

Han X, Zhao C, Wang S, Pan Z, Jiang Z, Tang X (2022) Multifunctional TiO2/C nanosheets derived from 3D metal–organic frameworks for mild-temperature-photothermal-sonodynamic-chemodynamic therapy under photoacoustic image guidance. J Colloid Interface Sci 621:360–373

Hasheminasab M, Bozorgnezhad A, Shams M, Ahmadi G, Kanani H (2014). Simultaneous investigation of PEMFC performance and water content at different flow rates and relative humidities. In: International conference on nanochannels, microchannels, and minichannels, American Society of Mechanical Engineers

He X, Jiang Z, Akakuru OU, Li J, Wu A (2021) Nanoscale covalent organic frameworks: from controlled synthesis to cancer therapy. Chem Commun 57(93):12417–12435

Hussaini H, Wang C (2022) Battery energy storage system control and integration strategy for the more electric aircraft DC grid application. Int J Hydromech 5(3):275–290

Jiang Z, Han X, Zhao C, Wang S, Tang X (2022) Recent advance in biological responsive nanomaterials for biosensing and molecular imaging application. Int J Mol Sci 23(3):1923

Kanani H, Shams M, Hasheminasab M, Bozorgnezhad A (2015) Model development and optimization of operating conditions to maximize PEMFC performance by response surface methodology. Energy Convers Manage 93:9–22

Ke F, Qiu L-G, Yuan Y-P, Peng F-M, Jiang X, Xie A-J, Shen Y-H, Zhu J-F (2011) Thiol-functionalization of metal-organic framework by a facile coordination-based postsynthetic strategy and enhanced removal of Hg2+ from water. J Hazard Mater 196:36–43

Kennedy IR, Hodzic M, Crossan AN, Crossan N, Acharige N, Runcie JW (2023) Estimating maximum power from wind turbines with a simple newtonian approach. Arch Adv Eng Sci 1(1):38–54

Kong L, Wang L, Li F, Li J, Wang Y, Cai Z, Zhou J, Guo J, Wang G (2023) Life cycle-oriented low-carbon product design based on the constraint satisfaction problem. Energy Convers Manage 286:117069

Leung SCE, Shukla P, Chen D, Eftekhari E, An H, Zare F, Ghasemi N, Zhang D, Nguyen N-T, Li Q (2022) Emerging technologies for PFOS/PFOA degradation: a review. Sci Total Environ 827:153669

Li B, Wang J, Nassani AA, Binsaeed RH, Li Z (2023a) The future of green energy: a panel study on the role of renewable resources in the transition to a green economy. Energy Economics 127:107026

Li H, Xu X, Liu Y, Hao Y, Xu Z (2023b) Fluorophore molecule loaded in Tb-MOF for dual-channel fluorescence chemosensor for consecutive visual detection of bacterial spores and dichromate anion. J Alloy Compd 944:169138

Li H, Wu Y, Xu Z, Wang Y (2024) In situ anchoring Cu nanoclusters on Cu-MOF: a new strategy for a combination of catalysis and fluorescence toward the detection of H2O2 and 2, 4-DNP. Chem Eng J 479:147508

Lin Z, Lv Z, Zhou X, Xiao H, Wu J, Li Z (2018) Postsynthetic strategy to prepare ACN@ Cu-BTCs with enhanced water vapor stability and CO2/CH4 separation selectivity. Ind Eng Chem Res 57(10):3765–3772

Liu C, Yang W (2022) Theoretical analysis and numerical study on a flexible piezoelectric wave energy converter. Int J Hydromech 5(4):292–310

Liu W, Huang F, Liao Y, Zhang J, Ren G, Zhuang Z, Zhen J, Lin Z, Wang C (2008) Treatment of CrVI-containing Mg (OH) 2 nanowaste. Angew Chem 120(30):5701–5704

Liu T-F, Zou L, Feng D, Chen Y-P, Fordham S, Wang X, Liu Y, Zhou H-C (2014) Stepwise synthesis of robust metal–organic frameworks via postsynthetic metathesis and oxidation of metal nodes in a single-crystal to single-crystal transformation. J Am Chem Soc 136(22):7813–7816

Liu T, Gu Y, Xing DY, Dong W, Wu X (2018) Rapid and high-capacity adsorption of PFOS and PFOA by regenerable ammoniated magnetic particle. Environ Sci Pollut Res 25:13813–13822

Liu K, Jiang Z, Lalancette RA, Tang X, Jäkle F (2022) Near-infrared-absorbing B-N lewis pair-functionalized anthracenes: electronic structure tuning, conformational isomerism, and applications in photothermal cancer therapy. J Am Chem Soc 144(41):18908–18917

Liu Z, Xu Z, Zhu X, Yin L, Yin Z, Li X, Zheng W (2023) Calculation of carbon emissions in wastewater treatment and its neutralization measures: a review. Sci Total Environ 912:169356

Lv Z, Wang H, Chen C, Yang S, Chen L, Alsaedi A, Hayat T (2019) Enhanced removal of uranium (VI) from aqueous solution by a novel Mg-MOF-74-derived porous MgO/carbon adsorbent. J Colloid Interface Sci 537:A1–A10

Ly A, El-Sayegh Z (2023) Tire wear and pollutants: an overview of research. Arch Adv Eng Sci 1(1):2–10

Lyu X-J, Liu Y, Chen C, Sima M, Lyu J-F, Ma Z-Y, Huang S (2020) Enhanced use of foam fractionation in the photodegradation of perfluorooctane sulfonate (PFOS). Sep Purif Technol 253:117488

Madden DG, O'Nolan D, Rampal N, Babu R, Çamur C, Al Shakhs AN, Zhang S-Y, Rance GA, Perez J, Maria Casati NP (2022) Densified HKUST-1 monoliths as a route to high volumetric and gravimetric hydrogen storage capacity. J Am Chem Soc 144(30):13729–13739

Meng P, Deng S, Wang B, Huang J, Wang Y, Yu G (2017) Superhigh adsorption of perfluorooctane sulfonate on aminated polyacrylonitrile fibers with the assistance of air bubbles. Chem Eng J 315:108–114

Mirabediny M, Sun J, Yu TT, Åkermark B, Das B, Kumar N (2023) Effective PFAS degradation by electrochemical oxidation methods-recent progress and requirement. Chemosphere 321:138109

Mohammadi N, Mousazadeh B, Hamoule T (2021) Synthesis and characterization of NH 2-SiO 2@ Cu-MOF as a high-performance adsorbent for Pb ion removal from water environment. Environ Dev Sustain 23:1688–1705

Mousazadeh B, Mohammadi N, Khosravi-Nikou M (2024) Synthesis and characterization of porous activated carbons derived from lotus nut and their performance for CO2 adsorption. Int J Environ Sci Technol 21:1–16

Pauletto PS, Florent M, Bandosz TJ (2023) On the directions of carbon surface modifications towards efficient PFOS removal: analyzing the interplay of porosity and surface chemistry. Chem Eng J 455:140897

Punyapalakul P, Suksomboon K, Prarat P, Khaodhiar S (2013) Effects of surface functional groups and porous structures on adsorption and recovery of perfluorinated compounds by inorganic porous silicas. Sep Sci Technol 48(5):775–788

Rayne S, Forest K (2009) Perfluoroalkyl sulfonic and carboxylic acids: a critical review of physicochemical properties, levels and patterns in waters and wastewaters, and treatment methods. J Environ Sci Health Part A 44(12):1145–1199

Ross I, McDonough J, Miles J, Storch P, Thelakkat Kochunarayanan P, Kalve E, Hurst J, Dasgupta SS, Burdick J (2018) A review of emerging technologies for remediation of PFASs. Remediat J 28(2):101–126

Shen Y, Sun P, Ye L, Xu D (2023) Progress of anaerobic membrane bioreactor in municipal wastewater treatment. Sci Adv Mater 15(10):1277–1298

Song Z, Han D, Yang M, Huang J, Shao X, Li H (2023) Formic acid formation via direct hydration reaction (CO+ H2O→ HCOOH) on magnesia-silver composite. Appl Surf Sci 607:155067

Verma H, Siruvuri SV, Budarapu P (2024) A machine learning-based image classification of silicon solar cells. Int J Hydromech 7(1):49–66

Wang C, Liu X, Demir NK, Chen JP, Li K (2016) Applications of water stable metal–organic frameworks. Chem Soc Rev 45(18):5107–5134

Wang H-C, Wang Y-Q, Wang X, Yin W-X, Yu T-C, Xue C-H, Wang A-J (2024a) Multimodal machine learning guides low carbon aeration strategies in urban wastewater treatment. Engineering 36:51

Wang Z, Yang P, He X, Yu Q (2024b) Preparation of intercalated MXene by TPAOH and its adsorption characteristics towards U (VI). J Radioanal Nucl Chem 333(4):1999–2014

Weiss A, Reimer N, Stock N, Tiemann M, Wagner T (2015) Surface-modified CAU-10 MOF materials as humidity sensors: impedance spectroscopic study on water uptake. Phys Chem Chem Phys 17(33):21634–21642

Xu P, Liu X, Zhao Y, Lan D, Shin I (2023) Study of graphdiyne biomimetic nanomaterials as fluorescent sensors of ciprofloxacin hydrochloride in water environment. Desalin Water Treat 302:129–137

Xue Y, Liu X, Zhang N, Shao Y, Xu CC (2023a) Enhanced photocatalytic performance of iron oxides@ HTCC fabricated from zinc extraction tailings for methylene blue degradation: Investigation of the photocatalytic mechanism. Int J Miner Metall Mater 30(12):2364–2374

Xue Y, Yang T, Liu X, Cao Z, Gu J, Wang Y (2023b) Enabling efficient and economical degradation of PCDD/Fs in MSWIFA via catalysis and dechlorination effect of EMR in synergistic thermal treatment. Chemosphere 342:140164

Yan T, Chen H, Jiang F, Wang X (2014) Adsorption of perfluorooctane sulfonate and perfluorooctanoic acid on magnetic mesoporous carbon nitride. J Chem Eng Data 59(2):508–515

Yan R, Lin Y, Yu N, Wu Y (2023) A low-carbon economic dispatch model for electricity market with wind power based on improved ant-lion optimisation algorithm. CAAI Trans Intell Technol 8(1):29–39

Yang S, Peng L, Sun DT, Asgari M, Oveisi E, Trukhina O, Bulut S, Jamali A, Queen WL (2019) A new post-synthetic polymerization strategy makes metal–organic frameworks more stable. Chem Sci 10(17):4542–4549

Yu F, Li C, Li W, Yu Z, Xu Z, Liu Y, Wang B, Na B, Qiu J (2024a) Π-Skeleton tailoring of olefin-linked covalent organic frameworks achieving low exciton binding energy for photo-enhanced uranium extraction from seawater. Adv Func Mater 34(1):2307230

Yu Z, Xu X, Guo L, Yuzuak S, Lu Y (2024b) Physiological and biochemical effects of polystyrene micro/nano plastics on Arabidopsis thaliana. J Hazard Mater 469:133861

Zhang Q, Deng S, Yu G, Huang J (2011a) Removal of perfluorooctane sulfonate from aqueous solution by crosslinked chitosan beads: sorption kinetics and uptake mechanism. Biores Technol 102(3):2265–2271

Zhang X, Niu H, Pan Y, Shi Y, Cai Y (2011b) Modifying the surface of Fe3O4/SiO2 magnetic nanoparticles with C18/NH2 mixed group to get an efficient sorbent for anionic organic pollutants. J Colloid Interface Sci 362(1):107–112

Zhang W, Hu Y, Ge J, Jiang H-L, Yu S-H (2014) A facile and general coating approach to moisture/water-resistant metal–organic frameworks with intact porosity. J Am Chem Soc 136(49):16978–16981

Zhang Z, Sarkar D, Biswas JK, Datta R (2022) Biodegradation of per- and polyfluoroalkyl substances (PFAS): a review. Biores Technol 344:126223

Zhao X, Fan B, Qiao N, Soomro RA, Zhang R, Xu B (2024) Stabilized Ti3C2Tx-doped 3D vesicle polypyrrole coating for efficient protection toward copper in artificial seawater. Appl Surf Sci 642:158639